Applied Radiation and Isotopes 125 (2017) 66–73

Contents lists available at ScienceDirect

Applied Radiation and Isotopes

journal homepage: www.elsevier.com/locate/apradiso

Development of tritiated nitroxide for nuclear battery

Johnny Russo[a,d,*], Marc Litz[a], William Ray II[a,b], Gerald M. Rosen[c], David I. Bigio[d], Robert Fazio[e]

[a] Sensors and Electron Devices Directorate, US Army Research Laboratory, Adelphi, MD 20783, USA
[b] Oak Ridge Associated Universities (ORAU), Oak Ridge, TN 37831, USA
[c] Department of Pharmaceutical Sciences, University of Maryland School of Pharmacy, Baltimore, MD 21201, USA
[d] Department of Mechanical Engineering, University of Maryland, College Park, MD 20742, USA
[e] Vitrax, Placentia, CA 92870, USA

ABSTRACT

Beta radioisotope energy sources, such as tritium (^{3}H), have shown significant potential in satisfying the needs of a sensor-driven world. The limitations of current beta sources include: (i) low beta-flux power, (ii) intrinsic isotope leakage and (iii) beta self-absorption. The figure of merit is the beta-flux power (dP_β/dS in $\mu W_n/cm^2$), where an optimal portion of incident beta particles penetrates the semiconductor depletion region. Thus, the goal of this research was to identify a compound to contain a beta emitter that can permit beta-flux power of at least 0.73 $\mu W_n/cm^2$ from one side, where it can be used for both planar and textured semiconductor structures. Nitroxides were chosen because of previous demonstrated deuteration, ease of synthesis, diversity of structure, and pliability. As a proof-of-principle, nitroxide [**1**] was prepared and tritiated with a specific activity of 103 Ci/g. The corresponding tritiated nitroxide in toluene was found to have no measurable $^3H_2$ outgassing after 27 days, thus it was considered stable. After 256 days in solution, analysis of the compound showed only 2% tritium loss, whereas in solid form, there was approximately 50% of tritium loss after 21 days. To compare with the performance of a typical metal tritide carrier, the standard MCNPX Monte Carlo code was used to calculate the beta-flux power of tritiated nitroxide and titanium tritide (0.2 $\mu W_n/cm^2$ and 0.70 $\mu W_n/cm^2$), respectively. The difference between numerical and empirical results of titanium tritide was 4%, showing the model validity. For the tritiated nitroxide to be comparable to titanium tritide in a planar configuration (2-D), the gravimetric density (^{3}H weighted percentage) would need to be at least 9%.

1. Introduction

There has been an increasing interest and use of autonomous sensors in environmental monitoring for space and terrestrial applications where operations over multiple decades are essential (Gasulla et al., 2014). Unfortunately, the sensor power requirements increase faster than the sensor volume. A sensor with compact size and high-energy consumption cannot maintain long-term operation, especially over decades. Chemical batteries are currently used as a provisional solution to this problem. However, chemical batteries are a limiting component, due to energy density, short lifetime (less than 10 years), and sensitivity to environmental conditions. Beta isotope batteries, however, can address these limitations. This energy source can provide maintenance-free power for the lifetime of the sensor using less than one cubic centimeter of volume.

Beta emitting isotopes are appealing candidates for energy sources compared to alpha and gamma emitters, as they do the least amount of harm to the semiconductor and environment. Tritium (^{3}H or T) and Nickel-63 (^{63}Ni) are used for several betavoltaic (βV) prototypes since they have low energy beta particles providing enhanced battery lifetimes due to the absence of semiconductor degradation (Bower et al., 2002). Presently, βV cells are the most efficient type of isotope battery with the lowest volume (Bower et al., 2002). They are direct-conversion systems, converting beta-radiation energy into usable electrical energy through semiconductor energy conversion. In general, they are typically more energy dense with semiconductor efficiencies ($\eta_{\beta\text{-}e}$) ranging from 1% to 20% depending on the radioisotope and converter type (Bower et al., 2002; Thomas et al., 2016; Li and Zhang, 2015; Tin and Lal, 2009). Typically, for betavoltaic prototypes, the semiconductor is solid, either planar or micromachined to increase surface power density of the betavoltaic cell (Guo et al., 2003). In addition to solid and high aspect ratio semiconductor structures, a liquid semiconductor was used in a nuclear microbattery prototype using selenium with a 166 MBq radioisotope of sulfur-35 and total conversion efficiency of 1.62% (Wacharasindhu et al., 2009).

Tritium is the isotope of choice for a βV cell since it is the least

* Corresponding author at: Sensors and Electron Devices Directorate, US Army Research Laboratory, Adelphi, MD 20783, USA.
E-mail address: johnnyru19@gmail.com (J. Russo).

http://dx.doi.org/10.1016/j.apradiso.2017.04.013
Received 12 January 2017; Received in revised form 24 March 2017; Accepted 4 April 2017
Available online 07 April 2017
0969-8043/

Nomenclature

2-D	two-dimensional
3-D	three-dimensional
A_m	specific activity
U.S. ARL	U.S. Army Research Laboratory
COTS	commercial-off-the-shelf
$D_{0.99}$	saturation thickness layer
D_L	optimal thickness layer
dP_β/dS	Beta-flux power, also called power density
EHPs	electron-hole pairs
FOM_{2D}	figure of merit of 2-D betavoltaic configuration
FOM_{3D}	figure of merit of 3-D betavoltaic configuration
η_f	fuel usage efficiency
GD	gravimetric density
GaN	gallium nitride
HPLC	high-performance liquid chromatography
MS	mass spectrometry
^{63}Ni	nickel-63
NO_x	nitroxide for tritiation
OED LLC	Organic Electronic Devices LLC
PDA	photodiode array
Sc^3H	scandium tritide
Ti^3H_x	titanium tritide/tritiated titanium hydride
^3H, T	tritium
S_m	effective surface activity
STP	standard temperature and pressure
η_s	system efficiency
V_m	volume activity (Ci/cm^3)

expensive isotope per kilogram and kilojoule of all beta-emitting radioisotopes, has low toxicity, is a low energy beta emitter, and has a half-life of 12.6 years (Moghissi et al., 1975). Nevertheless, there are constraints that restrict its application as an energy source. $^3H_2$ is a gas at STP, and it must be physically contained in a vessel or chemically bonded in a compound. The state-of-the-art approach is to store $^3H_2$ in metal foils forming a metal tritide (Kavetsky et al., 2002; Shpil'rain et al., 1983). The specific activity (A_m) of these compounds is approximately 1000 Ci/g. However, there are limitations with this approach relative to fuel usage efficiency (η_f), geometric constraints (film thickness and high aspect ratio structures), and effective surface activity. Reported beta-flux power (dP_β/dS) from a titanium tritide foil ($Ti^3H_{1.66}$) was approximately 0.73 $\mu W_n/cm^2$ (Thomas et al., 2016). Metal tritides are limited to a single side of beta emission collection, lowering the system efficiency (η_s) of the βV cell by approximately 50%.

Polymers, such as polystyrene, have previously been examined as potential carriers for tritium (Kavetsky et al., 2002). In other works, there was no attempt to calculate nor measure the beta-flux power, so the only metric of comparison with metal tritides is specific activity. Thus far, there are fluctuating theoretical specific activity results ranging from 50 Ci/g to 600 Ci/g, depending on the structures of labeled polymer (Kavetsky et al., 2002). Tritiated polystyrene produced in a benzene solution had specific activity of 50 Ci/g and 2.5 Ci/g as a solid due to $^3H_2$ outgassing (Kavetsky et al., 2002). p-Di(phenylethynyl) benzene was tritiated with a specific activity of 10 Ci/g (Renschler et al., 1989). And, polystyrene was tritiated with a specific activity of 150 Ci/g (Takagi et al., 1992). However, the authors neither measured $^3H_2$ outgassing nor determined the rate of degradation. In fact, the lack of these measurements suggests that the maximum specific activity, which was reported to be 50 Ci/g in solution, remains questionable. Thus, these low metrics eliminate polymers from being possible candidates for tritiated compounds.

A search of the literature indicated that nitroxides were an initial family of compounds worth exploring. These paramagnetic species are readily synthesized, allowing for diversity of structure, and most are solids at ambient conditions, all of which are important factors to consider for tritiation experiments (Burks et al., 2010a; Rosen et al., 1974; Rosen et al., 2002; Rosen et al., 1977; Eriksson et al., 1986). Moreover, nitroxides can be synthesized with lower molecular weights compared with polymers and are solid at standard ambient temperature and pressure (SATP), limiting beta self-absorption and offering various coating techniques for different surfaces. Finally, they have already been fully deuterated (Burks et al., 2010a).

Herein, the experimenters tritiated a model nitroxide for a micro-nuclear battery made up of βV cell arrays. As a proof-of-principle, we tritiated nitroxide ([**1**], Fig. 1). The tritiation afforded nitroxide [**2**] and trioxylamine [**3**] (Fig. 1) in which specific activity and stability (^3H percentage) were measured. Using theoretical equations, tritiated nitroxide [**2**] metrics were compared to metal tritides. Further, Monte Carlo simulations were performed to approximate optimal layer thickness (D_L) and beta-flux power (dP_β/dS). Results were validated through comparison with titanium tritide and nitroxide [**2**]. Finally, the ^3H gravimetric density (GD, wt% ^3H) required to be comparable to titanium tritides was identified by this numerical method.

2. Experimental, theoretical, and numerical methods

2.1. Nitroxide [1] synthesis and tritiation

The nitroxide, 4-methoxycarbonylmethylidene-2,2,6,6-tetramethyl-1-piperidinyloxyl ([**1**], Fig. 1) was prepared, as reported in the literature (Burks et al., 2010b). This compound was a viable candidate for the introduction of tritium atom (^3H), into the reaction at high-specific activity. The catalytic reduction of nitroxide [**1**] in methanol was initiated using one equivalent of Pd/C (10%) in the presence of $^3H_2$ (100 mCi). After the reaction was completed, the resultant solution was degassed, filtered, and the filtrate was then washed with additional methanol. The solution was then concentrated to dryness. This procedure was repeated twice more to ensure removal of unbound $^3H_2$. The crude product was dissolved in toluene and assayed for radioactivity. Radiochemical purity was assessed by reverse phase high-performance liquid chromatography (HPLC) adapted with an in-line radiochemical detector.

2.2. Stability procedure

The toluene solution containing tritiated mixture of compounds [**2**] and [**3**] was evaluated at 1, 7, 27, and 256 days, post-reduction. The sample was stored between measurements at −20 °C and 1 atm. After 27 days, a portion of reaction mixture was divided into three 8 mCi samples. Then, toluene was evaporated from the three samples. Each solid sample was analyzed at day 7, 14, and 21. At each time point, an analysis for radiochemical composition and tritium lability was performed using reverse phase HPLC, photodiode analysis (PDA). Solid

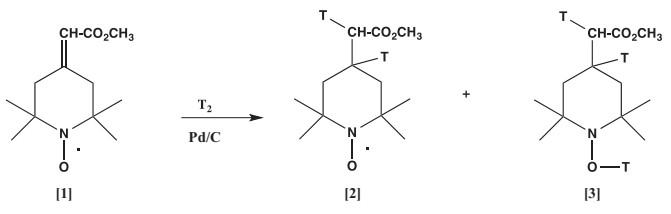

Fig. 1. Scheme 1 skeletal model of nitroxide tritiation. The precursor [1] (Burks et al., 2010b) was tritiated using catalyst and tritium gas (^3H = T). If the trioxylamine [3] is not held at vacuum and exposed to air, it will lose one tritium leaving a free electron, tritiated nitroxide [2].

samples were re-dissolved in toluene just prior to analysis.

2.3. Tritiated nitroxide [2] theoretical metrics

Tritiated compound metrics were measured and calculated at the beta flux saturation point, limited by layer self-absorption (Table 1). Equations were formulated to calculate the tritiation metrics based on the point beta source dose function and empirical data of thin-layer sources (Kavetsky et al., 2002). The FOM_{2D}s for planar (2-D) configuration are beta-flux power (dP_β/dS) and effective surface activity (S_m) exiting the compound surface given in Eqs. (1)–(4). The specific power parameter P_{sp} is calculated as

$$P_{sp} = 3.\ 7\times10^{10}\int_0^{\varepsilon_{max}} w(\varepsilon_\beta)\varepsilon_\beta d\varepsilon_\beta = 3.\ 7\times10^{10}\varepsilon_{av} = 5.92\varepsilon_{av} \quad (1)$$

where ε_β is the kinetic energy of beta particles, $w(\varepsilon_\beta)$ is the beta spectral distribution, 3.7×10^{10} is the normalizing factor to convert number of incident decays to Curie (Ci), and the ε_{av} is the average beta energy in spectrum. P_{sp} is the nuclear power per 1 Ci (μW_n/Ci). The mass absorption coefficient μ_m, in units of square centimeters per gram, is based on empirical data from titanium tritide-based sources, and used to calculate other tritiated compounds' FOM_{2D} (Table 1).

$$\mu_m = 15.\ 5\varepsilon_{max}^{-1.41}, \quad [\frac{cm^2}{g}] \quad (2)$$

$$\frac{dP_\beta}{dS} = \frac{A_m P_{sp}}{2(\mu_m)}\int_0^1 z[1-\exp((\mu_m\rho D_L)/z)]dz, \quad [\frac{W}{cm^2}] \quad (3)$$

$$S_m = \frac{\frac{dP_\beta}{dS}}{3.\ 7\times10^7 * \varepsilon_{av}[keV] * (1.\ 6\times10^{-16})}, [\frac{mCi}{cm^2}] \quad (4)$$

where ε_{max} is the maximum beta energy of isotope, D_L is the compound's optimal thickness layer, and ρ is the mass density. Beta-flux power (dP_β/dS) is the product of specific activity and beta source dose constant, $9\times10^{-4}\mu W_n{*}g/(Ci{*}cm^2)$ (Kavetsky et al., 2002). The constant includes specific power, mass absorption coefficient, and beta penetration depth factor. When comparing calculations with reported beta-flux power and surface effective activity results, there is less than a 7% difference for Sc^3H and $Ti^3H_{1.66}$ foils (Thomas et al., 2016; Liu et al., 2008). Differences in theoretical and experimental values are because of tritium concentration and loading percentage assumptions. These differences are unknown for organic compounds because there are no previous tritiation results. They have only been deuterated. The deuterium is substituted by tritium to calculate the parameters.

Equations (Kavetsky et al., 2002) were used to calculate tritiated nitroxides' FOM_{2D}s, but an additional method was required to approximate the optimal layer thickness of each tritiated nitroxide. The Continuously Slowing Down Approximation (CSDA) is used by the National Institute of Standards and Technology (NIST) ESTAR software to calculate the $D_{0.99}$ of tritiated nitroxide (ESTAR et al., 2016). ESTAR is a 1-D model that only identifies the 100% electron stopping range of a monoenergetic electron energy by calculating the total stopping power (T, eV*cm^2/g) (ESTAR et al., 2016). The input parameters are mass density and elemental composition. The average beta energy of ^3H used for the model was 5.7 keV. The ESTAR $D_{0.99}$ is calculated by using Eq. (5).

$$D_{0.99} = \left(\frac{\varepsilon_{av}[eV]}{T^*\rho}\right), \quad [\mu m] \quad (5)$$

where T is the total stopping power (eV*cm^2/g). ESTAR $D_{0.99}$ was compared to the theoretical and empirical $D_{0.99}$ of titanium tritide. Then, the ESTAR $D_{0.99}$ was compared to the empirical D_L of titanium tritide (Thomas et al., 2016). The tritiated nitroxide D_L is the product of the percent difference between the titanium tritide values (ESTAR $D_{0.99}$ and empirical D_L) and nitroxide ESTAR $D_{0.99}$ shown in Eq. (6).

$$D_{L,\ NO_x} = \left(\frac{D_{L,Ti^3H_x}}{D_{0.99,Ti^3H_x}}\right) * (D_{0.99,NO_x}), \quad [\mu m] \quad (6)$$

This equation assumed a similar relationship between each tritiated compound. The D_L approximation was used to the volume activity (V_m, Ci/cm^3) calculation, which is another important parameter for the micro-nuclear battery due to the volume limitation.

2.4. Numerical method

A numerical method was developed to approximate the FOM_{2D}s of tritiated nitroxide. Beta-flux power was calculated by Monte Carlo N-Particle eXtended (MCNPX) Transport Code modeling. It is a general-purpose MC code that has the capability to model neutron, photon, and electron (or coupled) transport. The software can simulate transportation of particles with energy from 1 keV to 100 MeV in materials. MCNPX can generate a more realistic model than the CSDA approach using more than one dimension, a full electron (beta) energy spectrum rather than simply the mean beta energy, the option to simulate isotropic beta emission from within a volume, and the ability to

Table 1
Theoretical calculations of tritiated compounds. Some of the values are averages due to tritiation yield fluctuations. Li^3H has the highest beta-flux power but is pyrolytic, eliminating it from comparison to other compounds. Metal tritides are widely used in current technologies but limited by beta range depth and planar beta emission.

Tritiated compound type	Specific activity (A_m) (Ci/g)	Mass density (ρ_m) (g/cm^3)	Gravimetric density (GD) (wt% ^{3}H)	Volume activity (V_m) (Ci/cm^3)	FOM_{2D} Beta-flux power at $D_{0.99}$ ($\frac{dP_\beta}{dS}$); $\left[\frac{\mu W_n}{cm^2}\right]$	Beta range depth ($D_{0.99}$) (μm)	Effective surface activity (S_m) (mCi/cm^2)
TiT_2 = Ti^3H_2	1100[a,b]	3.91[a,b]	4–12.5[a,b]	4300[a]	Max. 0.99[a] Exp. 0.73[c]	D_L = 0.40[c,d,e] $D_{0.99}$ = 0.77[a,b]	Max. (20)[a,c] Exp. (15)[c]
LiT = Li^3H	2910[a,b]	0.816[a,b]	25–30[a,b]	2317[a,b]	Max. 2.6[a,b]	$D_{0.99}$ = 3.7[a,b]	Max. (77)[a]
Tritiated organic compounds/polymers	100–1000[a]	1.0[a]	1–10[a]	100–1000[a]	0.09–0.90[a]	$D_{0.99}$ = 3.0[a]	Max. (27)[a]

Notes:
Organic compounds with $A_m \geq 500$ Ci/g have only been deuterated. The deuterium is substituted by tritium to calculate the parameters.
[Max. = maximum value based on theoretical calculations]
[Exp. = experiment results]
[a] Bower et al.
[b] Belovodskii et al.
[c] Thomas et al.
[d] Layer thickness (D_L) for betavoltaic cell following Thomas et al. approach.
[e] ESTAR calculations at average ^{3}H beta energy of 5.7 keV.

determine energy deposition profiles in structures (Pelowitz et al., 2011). Mohamadian et al. performed a geometrical optimization of GaN Betavoltaic Microbattery via Monte Carlo simulation, which identified the cylindrical array with the greatest performance (Mohamadian et al., 2007). The beta-radioisotope was electroplated ^{63}Ni thin film. There were two key reasons to embark on the modeling of tritiated nitroxide regions. The first was to calculate how much energy exits from a tritiated nitroxide region into the semiconductor converter. The second model goal was to calculate the required GD per nitroxide molecule to reach approximately 0.73 $\mu W_n/cm^2$ from a single side (planar configuration, 2-D). The gravimetric density (GD, wt% ^{3}H), the mass density, and chemical composition were parameters that affected the beta flux percentage exiting the compound surface.

The model was made up of three main cylinder structures in order of placement: nitroxide [**1**], tritiated nitroxide [**2**], and gallium nitride (GaN) bulk structure (Fig. 2). Although the layout was 3-D, the focus was on the 2-D interfaces between the regions. The GaN bulk structure represented the semiconductor converter in the βV cell (Litz et al., 2014). Nitroxide [**1**] was 100 μm thick with a 1-cm^2 area. The tritiated nitroxide [**2**] thickness was varied in simulations from 5 μm to 200 μm with an area of 1 cm^2. The molecular weight (M_w) was 235 g/mol. The GaN thickness was 100 μm with a 1-cm^2 area. The tritiated volume was divided for the simulation into 5 μm layers; GaN volume was divided into 100 nm layers. Energy deposition profiles and energy percentages exiting the tritiated volume into nitroxide [**1**] and GaN were the calculated within each layer. A $Ti^3H_{1.66}$ model was constructed using the same GaN volume dimensions to confirm the nitroxide model validity through comparison with $Ti^3H_{1.66}$ empirical data. The metal tritide volume was divided into 100 nm layers. The set of $Ti^3H_{1.66}$ layers had an increasing mass density, from 3.92 g/cm^3 to 4.1 g/cm^3 layer closest to the GaN component, to represent the reported metal tritide ^{3}H concentration profile (Thomas et al., 2016; Belovodskii et al., 1985).

3. Results and discussion

3.1. Nitroxide [1] synthesis and tritiation results

The goal of this research was to synthesize a small organic molecule that could be readily tritiated, the product of which would exhibit long-term stability and remain a solid to allow for easy formulation into a device as a proof-of-principle. A search of the literature suggested that nitroxide ([**1**], Fig. 1, Burks et al., 2010b) might meet these criteria. The synthesis of nitroxide [**1**] was not unduly difficult, allowing for sufficient amount to test our working hypothesis.

Mass spectrometry (MS) and reverse phase HPLC, PDA of the precursor were consistent with the assigned structure and validated the sample's purity (Fig. 3). After tritiation, the total radioactivity within the sample was 86 mCi. The specific activity was measured through MS analysis (25 Ci/mmol, 103 Ci/g). The achievable specific activity of 28% was limited by available $^3H_2$ present during radiation labeling (theoretical A_m = 365 Ci/g). Reverse phase HPLC profile (Fig. 4a) displays the presence nitroxide [**2**] at 7.66 min, and more polar product at 1.730 min, which based on reported catalytic reduction of nitroxides leads to the trioxylamine [**3**] (Rozantsev, 1970). If the sample is held under vacuum, three ^{3}H atoms react with the nitroxide [**1**], forming trioxylamine [**3**]. When the sample is not held in vacuum and exposed to air, the ^{3}H atom bonded to the oxygen on the 6-membered ring trioxylamine [**3**] can be lost, giving way to tritiated nitroxide [**2**] and free electron.

3.2. Stability

The solution stability results indicated little or no change regarding radiochemical composition or tritium lability (Figs. 4b and c). This was supported by the lack of any HPLC radiochemical profile change from day 1 through day 7. However, by day 27, there was a marked shift in the product distribution, with a loss of trioxylamine [**3**] and an increase in nitroxide [**2**] (Fig. 4c). This finding was expected as oxygen-containing solutions can mediate this one-electron oxidation affording a nitroxide (Patton et al., 1980). The fate of ^{3}H in this oxygen-containing toluene is unclear. However, by day 256, the solution containing the tritiated compound retained 94% of the initial ^{3}H content. Only 2% of ^{3}H was lost from degradation, when accounting for natural beta decay, which 96% would have remained after 256 days. This datum suggested that the total ^{3}H in the toluene solution was not lost, but ^{3}H most likely reacted either with itself or underwent an additional reaction.

Contrary to these findings, the solid stability analysis revealed a significant change in radiochemical composition after 7 days, with concomitant ^{3}H lability of about 50% (Table 2). The solid analysis results after 14 and 21 days were virtually unchanged after 7 days. After 7 days, there were additional peaks in the profile, which meant that other compounds were being formed due to degradation and ^{3}H loss. The tritiated nitroxide [**2**], at 7.67 min, started decreasing in intensity as an unknown compound with a retention time of 10.65 min appeared (Fig. 5). It has not been confirmed whether ^{3}H was lost during drying procedures from solution to solid or during the 7-day exposure of the solid under standard ambient temperature and pressure SATP. The solution sample must be heated to remove toluene, leaving just the tritiated sample. Since the remaining solid was stored at SATP, exposure to air may cause oxidation, producing free radicals, and leading to sample degradation. For primary beta-radiation effects, the solid form has a much greater concentration of tritium compared to tritiated compound in solution. Closer tritium proximity increases beta particle interaction without the toluene medium. A single beta particle can generate several diverse, reactive species that may impact the stability of the tritiated nitroxide [**2**] and trioxylamine [**3**].

The results of solid and solution stability were not surprising, when compared to other high specific activity tritiated, small organic compounds and polymers. Previously, ^{3}H-labeled polymers showed similar characteristics at specific activities greater than 10 Ci/g, when comparing solid versus solution stability. An example of this was reported, where tritiated polystyrene maintained a specific activity of 50 Ci/g in solution, while in solid form the specific activity was reduced to 2.5 Ci/g (Kavetsky et al., 2002). To date, specific activities for small organic compounds and polymers have been limited to approximated 10 Ci/g. Our initial trial yielded a tritiated nitroxide and trioxylamine at a specific activity five times above that previously reported (Kavetsky et al., 2002; Renschler et al., 1989). The experimenters are currently synthesizing a new family of nitroxides, which they believe will be the

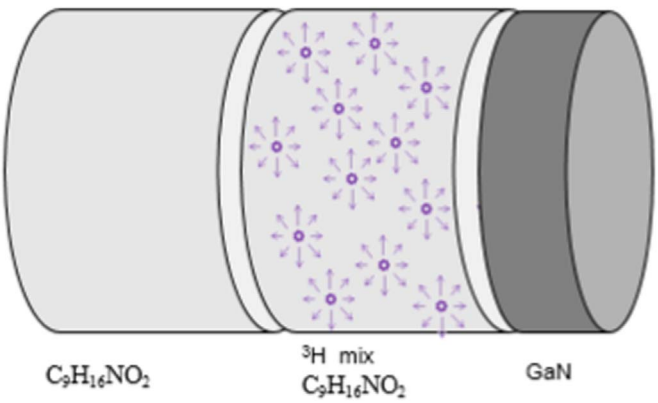

Fig. 2. Cylindrical layers representing the tritiated nitroxide [2] (^{3}H mix $C_9H_{16}NO_2$) region surrounded by GaN energy converter and untritiated nitroxide [1] ($C_9H_{16}NO_2$) regions. Parametric study of tritium loaded layer thickness was modelled using MCNPX. Although three-dimensional, the focus was on the 2-D interfaces between media and on thin layers.

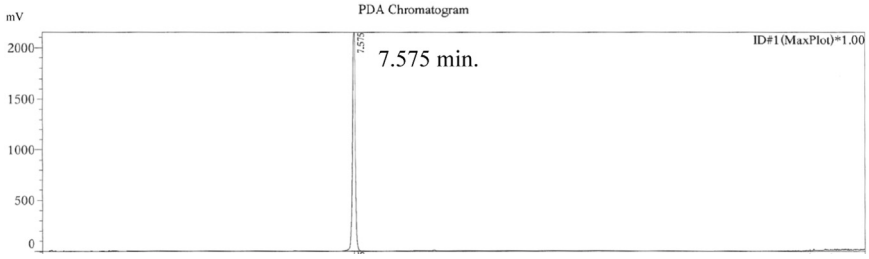

Fig. 3. A PDA chromatogram of precursor ([1], Fig. 1), obtained by reverse phase HPLC analysis to measure sample purity. The 7.575 min retention time peak (*x*-axis) represents the precursor [1] (*b*. Burks et al., 2010a, 2010b). The y-axis (mV) is the millivolt units measured by the PDA.

next generation of tritiated organic compounds that will exhibit high specific activity and long-term stability.

3.3. Tritiated nitroxide [2] theoretical metrics

The theoretical metrics were based on equations, assumptions, and ESTAR results explained in Section 2.3. These metrics were calculated

Table 2
Tritium content in each solid sample.

Tritiated sample	[^{3}H% content] (%)
Sample 1. 7 days	53
Sample 2. 14 days	58
Sample 3. 21 days	55

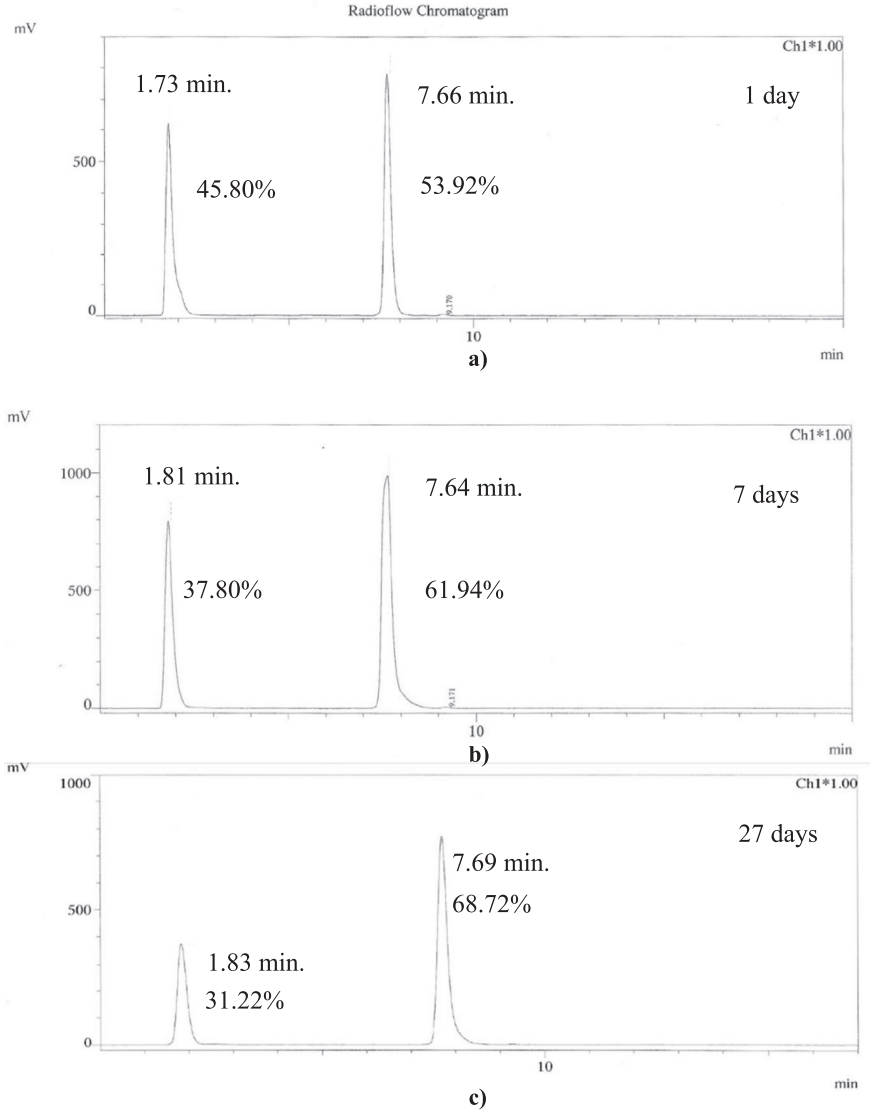

Fig. 4. Radioflow chromatograms of the tritiated nitroxide [2] and trioxylamine [3] in toluene after (a) 1, (b) 7, and (c) 27 days by reverse phase HPLC analysis. (a) The peak at 7.66 min is the tritiated nitroxide (Fig. 1 [2]). The peak at 1.73 min is the trioxylamine. The x-axis is retention time (min) and y-axis is in millivolt units. The compound in solution was completely stable with little or no degradation or tritium loss after 27 days. The trioxylamine [3] concentration started reducing from 45.80% to 31.28%, while the tritiated nitroxide increases from 53.92% to 68.72% from (a) 1 to (c) 27 days. This phenomenon was caused by the oxidation of the sample inside the toluene, where the trioxylamine [3] loses the tritium atom when exposed to oxygen, transforming into nitroxide [2], 7.69 min.

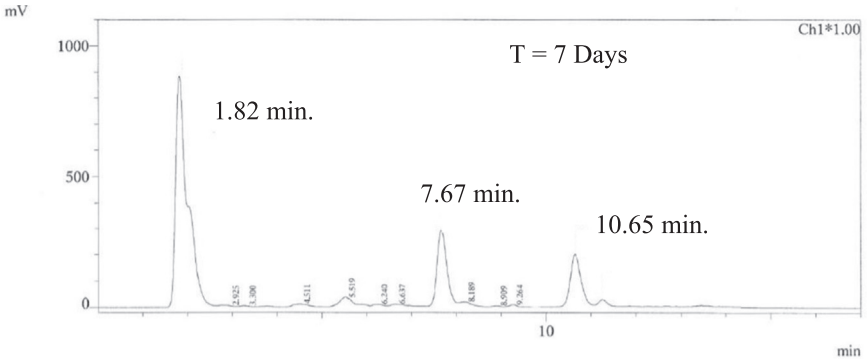

Fig. 5. A radioflow chromatogram of the tritiated nitroxide [2] (7.67 min) and trioxylamine [3] (1.82 min), and unknown product (10.65 min) as a solid after 7 days by reverse phase HPLC analysis. An additional peak is shown in the profile, which means that other compounds were being formed due to degradation and tritium loss.

Table 3
Theoretical calculations of tritiated nitroxides. FOM_{2D}'s account for one side of the tritiated layer. Parameters are calculated using equations in Bower et al. (2002).

Tritiated compound type	Specific activity (A_m) (Ci/g)	Mass density (ρ_m); (g/cm^3)	Gravimetric density (GD) (wt% ^{3}H)	Volume activity (V_m) (Ci/cm^3)		FOM_{2D} Beta-flux power at $D_{0.99}$ ($\frac{dP_\beta}{dS}$); $[\frac{\mu W_n}{cm^2}]$	Beta range depth (D_L)[a,b] (μm)	Effective surface activity (S_m) (mCi/cm^2)
Tritiated nitroxide [2]	365	0.1	3.83	36.5	0.33		12[a,b]	6.72
^{3}H at STP	9700[c]	2.68E−4[c]	100[c]	2.60[c]	8.73[c]		2623.5[b,c]	100[c]

[a] Layer thickness (D_L) for betavoltaic cell following Thomas et al. approach.
[b] ESTAR calculations at average ^{3}H beta energy of 5.7 keV.
[c] Bower et al. (2002).

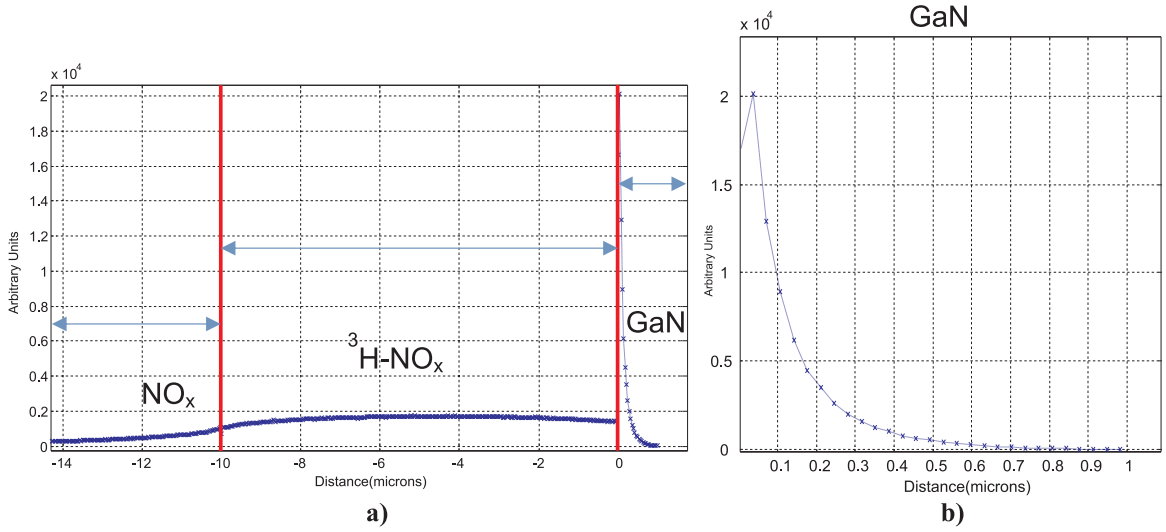

Fig. 6. (a) Energy deposition per gram of material profile across the three layers of sample. In this profile, tritiated nitroxide [2] (^{3}H-NO$_x$) in the center is 10 μm, GaN (right) is 50 μm, and nitroxide [1] (left) is 100 μm thick. The tritiated nitroxide [2] is surrounded on both sides, and β-energy deposited in each region is quantified to confirm conservation of energy during the simulation. Note: nitroxide = NO$_x$ and tritiated nitroxide = ^{3}H-NO$_x$. (b) Expanded view of energy deposition in GaN shows exponential absorption in GaN energy converter.

by substituting H and ^{2}H from previous experiments with ^{3}H (Burks et al., 2010a, 2010b). The electron range ($D_{0.99}$) for titanium tritide was 532 nm at 5.7 keV. The optimal thickness is 400 nm (Table 1) (Thomas et al., 2016). This thickness was 25% less than the ESTAR $D_{0.99}$ thickness. This factor was accounted for to calculate the tritiated nitroxide's D_L and FOM_{2D}s at a theoretical GD of 3.83 wt% ^{3}H. The specific activity and beta flux power (power density) of 365 Ci/g and 0.33 μW$_n$/cm^2 (6.73 mCi/cm^2) were less than the ^{3}H$_2$ metrics at SATP (Table 3). However, the tritiated nitroxide volume activity (V_m, Ci/cm^3) is 10 times greater than ^{3}H$_2$ metric, confirming it to be a more suitable beta source for a micro-nuclear battery.

3.4. Numerical method

Energy deposition profiles calculated from the MCNPX models showed that all beta energy is stopped within 1.5 μm of GaN and 50 μm of nitroxide [**1**] (Fig. 6). The tritiated nitroxide [**2**] was 10 μm deep. The beta energy deposition profile across the surrounding GaN and nitroxide [**1**] layers is shown in Fig. 6. The energy deposited in the 50 μm GaN structure volume adjacent to 10 μm tritiated nitroxide layer was summed, resulting in 11.5% of source activity. Beta energy escaping into the surrounding GaN and nitroxide regions accounted for 23% of the total energy originally deposited in the tritiated nitroxide volume. A parametric study of tritiated nitroxide thickness was performed to quantify the decreasing energy efficiency, which the ratio of energy deposited in surrounding layers and energy remaining in

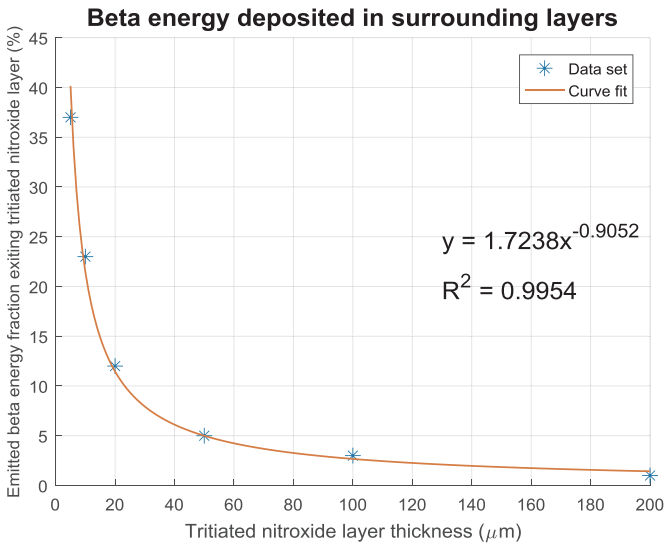

Fig. 7. The ratio of beta (β)-energy deposited in the surrounding layers (GaN and ^{3}H-NO$_x$-only) is compared to the β-energy exiting tritiated nitroxide surfaces (top and bottom) as function of its thickness.

Fig. 8. Model block diagram of radioactivity (Ci) calculation for tritiated nitroxide and titanium tritide volumes.

tritiated nitroxide [**2**] layer. The resulting decrease in energy release as a function of thickness of tritiated nitroxide layer shown in Fig. 7. A 5 μm thick layer of tritiated nitroxide of density 0.10 g/cm^3 released 38% into the surrounding layers.

The calculated radioactivity of the tritiated nitroxide volume (10 μm × 1 cm^2) was 50 mCi (Fig. 8). With this information, we determined the optimal thickness with the effective surface activity necessary to exceed the presently available Ti^{3}H$_{1.66}$ foils. The effective surface activity and beta-flux power was approximately 6 mCi/cm^2 and 0.2 μW$_n$/cm^2, respectively, with a D_L of 10 μm. These FOM_{2D} account for emission from a single side of the tritiated layer. To reach at least 0.73 μW$_n$/cm^2 for a single layer side, the GD would need to be at least 9 wt% ^{3}H. This is necessary for the tritiated nitroxide to reach a comparable beta-flux power to published values for metal tritides using a planar configuration. Nevertheless, when projecting to a 3-D configuration, the nitroxide may be more advantageous than metal tritides since more beta emission can be captured and converted from all sides of the layer. The nitroxide has a low mass density and homogenous ^{3}H concentration compared to metal tritide foils. These attributes would increase fuel efficiency above 50%, thus increasing a βV cell's system efficiency. Beta emission from metal tritide foils can only be captured from a single side due to beta self-absorption from foil backside. Also, ^{3}H concentration is not consistent throughout foil. A MCNPX model of Ti^{3}H$_{1.66}$ was formulated to check the tritiated nitroxide model validity. The titanium tritide volume was 400 nm × 1 cm^2. The total radioactivity was 169 mCi (Fig. 8). The percent of energy leaving the metal tritide layer was 10.35% from each side. The effective surface activity was 0.7 μW$_n$/cm^2, which represented an 81% loaded layer. This value was 4.1% lower than empirical value at 0.73 μW$_n$/cm^2. Experimental measurement error and MCNPX model assumptions, i.e. mass density gradient, contributed to the difference between results.

4. Conclusion

Nitroxide [**1**] was identified as a potential tritiated media for βV cells. It was selected for tritiation because of high deuteration and hydrogenation synthesis yield, low mass density, and pliability for application semiconductor structures (e.g., planar, micro-pillars). As a proof-of-principle, nitroxide [**1**] was tritiated with a specific activity of 103 Ci/g in solution and solid with a total radioactivity of 86 mCi. The solution, containing tritiated nitroxide [**1**] in toluene, lost nearly zero ^{3}H after 27 days and 2% after 256 days, while the solid form had approximately 50% ^{3}H loss plateau at 7 days, which value was stable at subsequent measurement times. With the first tritiation experiment, the experimenters were able to achieve the highest specific activity for an organic compound. A MCNPX model calculated a beta-flux power of approximately 0.2 μW$_n$/cm^2 (6 mCi/cm^2) for the tritiated nitroxide from one side of the 10 μm layer, which was nearly half the value of theoretical equations' metrics in Section 2.3. A 4.1% difference between numerical and empirical results with the same approach was identified for titanium tritide, establishing the validity of the approach. There were differences between numerical and theoretical calculations due to the mass absorption coefficient and other parameters based on titanium tritide empirical results. The model confirmed that a minimum of 9 wt % ^{3}H atoms per nitroxide would need to be achieved to reach 0.73 μW$_n$/cm^2 from one side. Numerical results, high experimental tritiation yield (86%), and limited ^{3}H loss (≈2% in solution and ≈50% in solid) encourages further investigation and tritiation of nitroxide compounds to reach higher power densities for micro-nuclear battery.

Acknowledgement

The authors wish to thank Dr. James J. Carroll, U.S. ARL, for valuable discussions and suggestions on numerical method and potential applications.

References

ESTAR: Stopping-power and range tables for electrons, NIST: Physical Meas. Laboratory, [Online]. Available: ⟨http://physics.nist.gov/PhysRefData/Star/Text/ESTAR.html⟩.
Belovodskii, L., Gaevoi, V., Grishmanovskii, V., 1985. "3H," Energoatomizdat, Moscow.
Bower, K.E., Barbanel, Y.A., Shreter, Y.G., 2002. Polymers, phosphors, and voltaics for radioisotope microbatteries. CRC Press, Boca Raton (USA).
Burks, S.R., Bakhshai, J., Makowsky, M.A., Muralidharan, S., Tsai, P., Rosen, G.M., Kao, J.P.Y., 2010a. 2H,15N-substituted nitroxides as sensitive probes for electron paramagnetic resonance imaging. J. Org. Chem. 75 (19), 6463–6467.
Burks, S.R., Makowsky, M.A., Yaffe, Z.A., Hoggle, C., Tsai, P., Muralidharan, S., Bowman, M.K., Kao, J.P., Rosen, G.M., 2010b. The effect of structure on nitroxide EPR spectral Linewidth,". J. Org. Chem. 75 (14), 4737–4741.
Eriksson, U.G., Tozer, T.N., Sosnovsky, G., Lukszo, J., Brasch, R.C., 1986. Human erythrocyte membrane permeability and nitroxyl spin-label reduction. J. Pharm. Sci. 75 (4), 334–337.
Gasulla, M., Penella, M.T., Lopez-Lapena, O., 2014. "Chapter 88: Powering AutonomousSensors," in Measurement, Instrumentation, and Sensors Handbook, Second Edition: spatial, Mechanical, Thermal, and Radiation Measurement. CRC Press, Hoboken, Taylor and Francis, pp. 88-1–88.11.
Guo, H., Lal, A., 2003. Nanopower betavoltaic microbatteries, Transducers, Solid-State Sensors, Actuators and Microsystems, 12th International Conference on.
Kavetsky, A.G., Nekhoroshkov S.N., Meleshkov, S.P., Kaminski, Y.L., Akulov G.P., Bower, K.E., 2002. Radioactive materials, ionizing radiation sources, and radioluminescent light sources for nuclear batteries. In: Polymers, Phosphors, and Voltaics for Radioisotope Microbatteries. CRC, Boca Raton, FL pp. 2, 6-40.
Li, M.G., Zhang, J., 2015. "A Betavoltaic Microcell Based on Semiconducting Single-walled Carbon Nanotubes Arrays/Si Heterojunctions. In: Proceedings of the 28th IEEE International Conference on Micro Electro Mechanical Systems (MEMS).
Litz, M., 2014. "Monte Carlo Evaluation of Tritium Beta Spectrum Energy Deposition in Gallium Nitride (GaN) Direct Energy Conversion Devices,"ARL-TR-7082, Adelphi, Maryland, September.
Liu, B., Chen, K.P., Kherani, N.P., Zukotynski, S., Antoniazzi, A.B., 2008. Betavoltaics using scandium tritide and contact potential difference. Appl. Phys. Lett. 92.
Moghissi, A.A., Carter, M.W., 1975. Tritium, Oak Ridge, TN: Oak Ridge National Laboratory.
Mohamadian, M., Feghhi, S.A.H., Afariadeh, H., 2007. Geometric optimization of GaN Betavoltaic Microbattery, Proceedings 7th WSEAS Intern. Conference on Power Sys.
Patton, S.E., Rosen, G.M., Rauckman, E.J., 1980. Superoxide production by purified hamster hepatic nuclei. Mol. Pharmacol. 18, 588–593.
Pelowitz, D., 2011. "MCNPX User's Manual Version 2.7.0 LA-CP-11-00438," Los Alamos National Laboratory.
Renschler, C.L., Clough, R.L., Shepodd, T.J., 1989. "Demonstration of completely organic, optically clear radioluminescent light," Sandia National Laboratories, Livermore, California and Albuquerque, New Mexico, 26 July.
Rosen, G.M., 1974. Use of Sodium cyanoborohydride in the preparation of biologically

active nitroxides. J. Med. Chem. 17 (3), 358–360.
Rosen, G.M., Rauckman, E.J., Hord, W.W., 1977. Spin-labeled TMA analogs as probes to study the anionic site of acetylcholinesterase. General. Pharmacol.: Vasc. Syst. 8 (5–6), 355–357.
Rosen, G.M., Schneider, E., Shortkroff, S., Tsai, P., Winalski, C.S., 2002. Use of sodium triacetoxyborohydride in the synthesis of nitroxide biradicals. J. Chem. Soc. 1, 2663–2667.
Rozantsev, E., 1970. Free Nitroxyl Radicals. (in) Plenum Press, New York, pp. 93–99.
Shpil'rain, E.E., Yakimovich, K.A., Mel'nikova, T.N., Polishchuk, A.Y., 1983. Therophysical Properties of Lithium Hydride, Deuteride, and Tritide and of Their Solutions with Lithium. American Institute of Physics Translation Series, New York.
Takagi, M., Norimatsu, T., Yamanaka, T., Nakai, S., 1992. Fabrication of deuterated-tritiated polystyrene shells for laser fusion experiments by means of an isotope exchange reaction. J. Vac. Sci. Technol. A 10, 239–242.
Thomas, C., Portnoff, S., Spencer, M.G., 2016. High Efficiency 4H-SiC betavoltaic power sources using tritium Radioisotope. Appl. Phys. Lett. 108.
Tin, S., Lal, A., 2009. A Radioisotope-powered surface acoustic wave transponder. J. Micromech. Microeng. 19 (9).
Wacharasindhu, T., et al., 2009. Radioisotope microbattery based on liquid semiconductor. Appl. Phys. Lett. 95, 014103.